STAG: Smart Tools and Applications in Graphics (2017)
A. Giachetti, P. Pingi and F. Stanco (Editors)

Visual analysis of glycogen derived lactate absorption in dense and sparse surface reconstructions of rodent brain structures

C. Calì[1], M. Agus[2], N. Gagnon[1], M. Hadwiger[2], and P. J. Magistretti [1]

[1] King Abdullah University of Science and Technology (KAUST)
Biological and Environmental Science and Engineering (BESE), Thuwal 23955-6900, Saudi Arabia
[2] King Abdullah University of Science and Technology (KAUST)
Visual Computing Center (VCC), Thuwal 23955-6900, Saudi Arabia

Abstract

Astrocytes are the most abundant type of glial cells of the central nervous system; their involvement in brain functioning, from synaptic to network level, is to date a matter of intense research. A well-established function of astroglial cells, among others, is the metabolic support of neurons. Recently, it has been shown that during tasks like learning and long-term memory formation, synapses sustain their metabolic needs using lactate, a compound that astrocytes can synthesize from glycogen, a molecule that stores glucose, rather than glucose itself. Aforementioned role of astrocytes, as energy reservoir to neurons, is challenging the classic paradigms of neuro-energetic research. Understanding their morphology at nano-scale resolution is therefore a fundamental research challenge with enormous implications on many branches of neuroscience research, such as the study of neuro-degenerative and cognitive disorders. Here, we present an illustrative visualization technique customized for the analysis of the interaction of astrocytic glycogen on surrounding neurites in order to formulate hypotheses on the energy absorption mechanisms. The method integrates a high-resolution surface reconstruction of neurites and the energy sources in form of glycogen granules, and computes an absorption map according to a radiance transfer mechanism. The technique is built on top of a framework for processing and rendering triangulated surface models, and it is used for real-time 3D exploration and inspection of the neural structures paired with the energy sources. The resulting visual representation provides an immediate and comprehensible illustration of the areas in which the probability of lactate shuttling is higher. This method has been further employed for testing neuroenergetics hypotheses about the utilization of glycogen during synaptic development.

Categories and Subject Descriptors (according to ACM CCS): J.5.1 [Human Centered Computing]: Visualization/Visualization techniques—Heat maps J.5.2 [Human Centered Computing]: Visualization/Visualization application domains—Scientific visualization

1. Introduction

Neuroscience is an exciting and challenging field of research, requiring a multidisciplinary effort from a large number of individuals and institutions from all over the world. In-depth understanding of the human brain structure and behavior would ultimately help to achieve important challenges for mankind, such as treat brain related disorders, or create computation device whose logic is inspired by human brain learning mechanisms [KMM*13]. Physiological mechanisms can be investigated at several spatial-temporal resolution. For instance, the molecular level characterizes how single molecules impact brain functioning at multiple scales; the cellular level focuses on understanding the functioning and morphology of individual cell types; the network and behavioral level investigates the connectivity of distinct neural circuits, and how these systems work together to make decisions and perform actions. Among the various topics of interest in the field, neuroenergetics is raising attention; manipulation of brain energy metabolism can have an impact on the normal physiological pace of the brain, and its dysfunction has been identified as one possible cause of neurodegenerative diseases. In short, neuroenergetics focuses on the mechanisms of energy storage and utilization in the brain at various levels [MA15]. One important source of energy is glycogen, an electron-dense molecule that is formed by glucose molecules. In order to locate and quantify these energy sources, researchers are taking advantage on high-resolution electron microscopy techniques, such as FIB-SEM or serial block face SEM [TG16], allowing to acquire brain samples at nanometer resolution and perform morphological analysis on the distribution on glycogen particles [CBB*16]. However, visual methods aimed to investigate and understand the brain energy metabolism at molecular and cellular levels are still at an early stage of development due to the complexity, and the resolution of the datasets. To date, neuroscientists commonly use standard mod-

DOI: 10.2312/stag.20171224

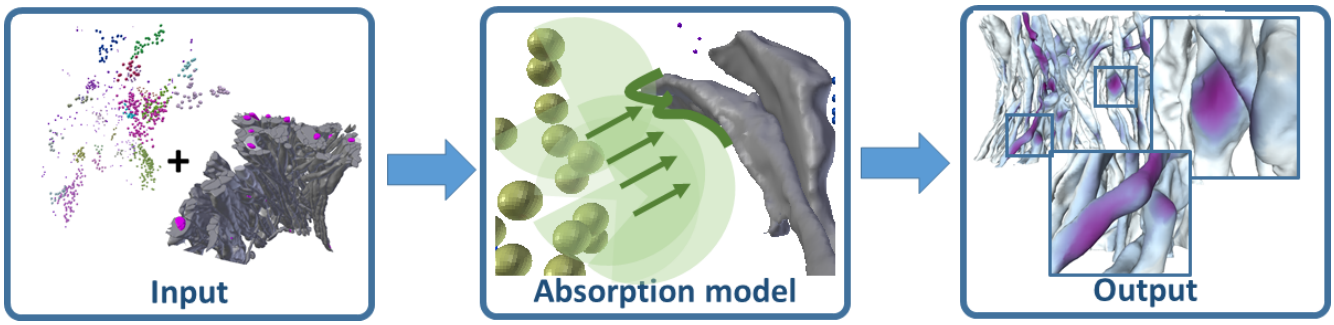

Figure 1: ***Method overview:*** *from 3D neurite models and a list of glycogen granules, our method computes the absorption rate of glycogen generated lactate according to a radiance transfer mechanism.*

eling software, and customize for morphometric analysis to study the distribution of glycogen compared to synaptic elements in the brain. [CBB*16]. We present here an illustrative visualization method suited for the interactive visual analysis of the influence of glycogen on surrounding neurites, namely axons and dendrites, as well as their synaptic elements, boutons and spines, respectively, in the interest of understanding the shuttling mechanisms of lactate [MWE*16]. The method takes as input a high-resolution surface reconstruction of neural structure and a list of energy sources in the form of glycogen granules, and computes an influence map according to a radiance transfer mechanism (see Figure 1). By considering a photon mapping analogy, areas of greater glycogen concentration will highlight portions of the cellular plasma membranes where the glycogen-derived lactate shuttling is more likely to occur. This framework can be used by neuroscientists for testing neuroenergetics hypotheses about the utilization of glycogen derived energy. Moreover, dense reconstruction of brain structures is a complex and time consuming process as each individual component needs to be imaged, identified and segmented. Rather, this method can be used for a preliminary selection of the neurites and, according to the absorption peaks, efforts can be focused on the areas of interest. The technique has been successfully used for the analysis of various surface reconstructions of electron microscopy stacks of rodent brains.

2. Related work

Neuroscience domain: astrocytes and glycogen metabolism role. It is generally acknowledged how astrocytes play a number of pivotal roles in the support of neuronal functioning throughout one's life-time. Astrocytes are involved in a variety of processes in the brain including fine tuning of synaptic transmission [CMS*09], neuroprotection and neurometabolism [MA15], however the underlining mechanism for these processes is far from being fully understood. Moreover, the recent discovery of the astrocyte neuron lactate shuttle (ANLS) has proved quintessential among astrocytes various unknown functions [BAM11, MA15]. This hypothesis illustrates how lactate is delivered to neurons during intense synaptic activity, and moreover glycogen-derived lactate has been related to one of the most important physiological brain functions, memory formation [SSB*11]. Despite its importance in both energy metabolism and memory, characterization of brain glycogen distribution has not been fully addressed. Recently, Oe et al. [OBA*16] investigated cerebral glycogen in mice using light microscopy and immunohistochemistry (IHC), and they observed a punctate distribution localized predominantly in astrocytic processes. With respect to the intra-cellular distributions, Cali et al. [CBB*16] observed that glycogen is localized primarily in small processes and clustered around boutons and spines. More investigation efforts are needed at addressing how other physiological processes other than learning, like for instance aging, are related to modifications in glycogen clustering and how this might be involved in declined memory abilities. Morphological studies are required to evaluate the influence of glycogen distribution compared to the surrounding neuronal structures (dendrites, axons and boutons) under several conditions. We propose here an illustrative analysis model aimed at easing morphological analysis of the distributions of glycogen on high resolution 3D reconstructions from micrometer resolution electron microscopy stacks of rodents brain samples.

Morphology visual analysis. The general workflow for 3D reconstruction and visual analysis of brain morphology (see Figure 2) begins with sample preparation and serial block face scanning electron microscopy (SEM) [KMWL08] imaging. Acquisition of biological tissues can be performed automatically at a z-resolution of 5-50 nanometers depending on the cutting technique [KMWL08]. After SEM, image processing for 3D reconstruction of the various cellular structures is performed on ultrastructural 3D datasets [BH16] by means of manual or semi-automatic segmentation techniques [KVRKB*15, BBH15]. Following registration and digital reconstruction, the 3D dataset can be explored and analyzed with a variety of tools that offer visualization and annotation. Currently many neuroscientists take advantage of commercial or free software solutions [CSS*12, SMGL*16, SSKH11] for 3D segmentation and reconstruction, and develop custom plug-ins for specific statistical and morphometric analysis [CBB*16, OBA*16, ACW*15, JNC*15]. Similarly, tools for visual analysis directly relying on segmented volume data are gaining visibility with the emergent field of connectomics [PKB*12]. They are mainly designed to explore the reconstructions of nanoscale neuronal connectivity for the interactive visual analysis using a dynamic-driven query approach [BAAK*13]. Our technique is an illustrative model that can be easily integrated into existing visual

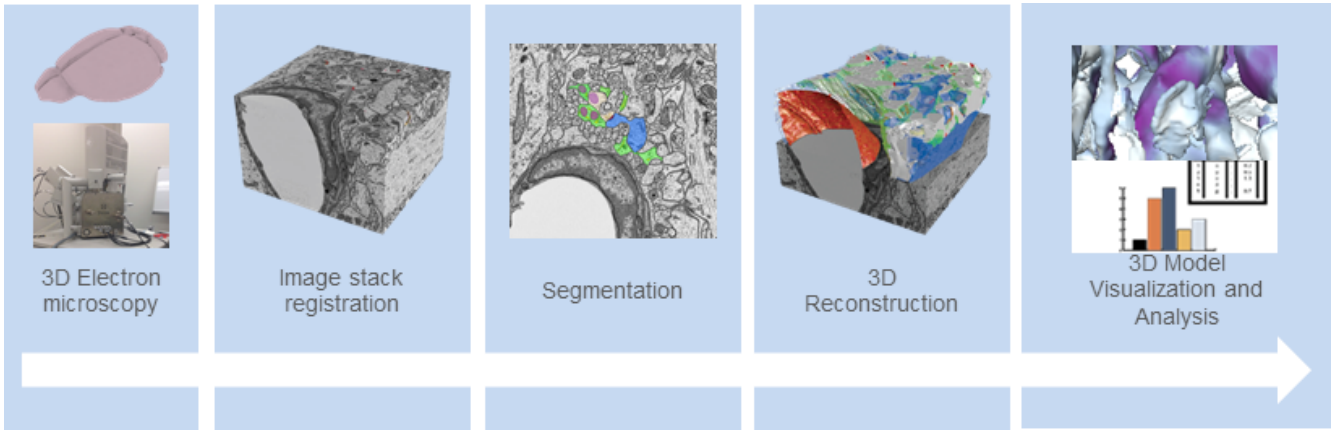

Figure 2: ***Workflow for morphology visual analysis:*** *starting from Serial Electron Microscopy imaging of brain samples, high resolution 3D models are computed from registered and segmented stacks of images and used as input for visualization and analysis tools.*

analysis frameworks, and can be used to analyze the density distributions of glycogen and other granules.

Density mapping in 3D structures. Mapping density distributions to a visual attribute, such as color, is a common practice in visualization. The Allen Brain Atlas viewer [LNT*08] maps density and level of gene expression to size in 3D and color respectively. BrainNet Viewer [XWH13], renders a voxel-based network using volume-to-surface mapping. Pycortex [GHLG15], uses a pixel-based mapping to render voxels true to form. Goddard et al. [GHF07] describe interactive methods for visualizing density maps using colors and by fitting atomic models. Recently, Agus et al. [AMB*17] have shown how density maps can be used to derive points of interest in work of arts in digital museums by tracking the users viewing positions. Our illustrative method is also related to photon map rendering techniques, which have been popularized in ray tracing [JC95b], shadow rendering [JC95a] and global illumination [Jen96]. Importance maps [PP98] are used to guide the emission of energy packets. In our model, we use a radiance transfer mechanism aimed to compute the influence of glycogen granules to nearby neurites.

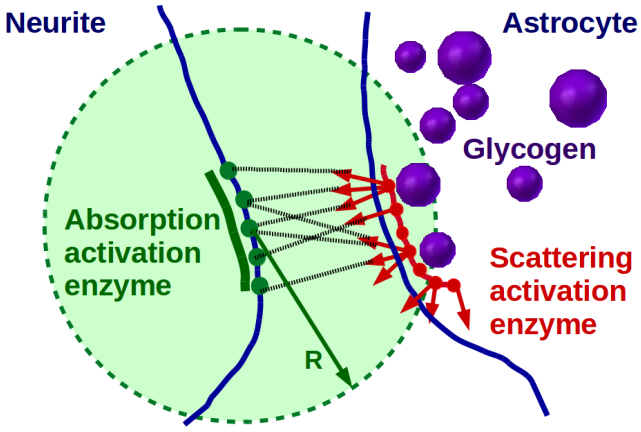

Figure 3: ***Glycogen absorption model scheme:*** *energy packets are scattered from glycogen granules according to the size, and presence of activation enzymes. Absorbed energy is computed on per-vertex basis with respect to the presence of absorption enzymes and a distance threshold.*

3. Glycogen Lactate Absorption Model

The proposed illustrative model highlights regions of astrocyte-and-neurite membranes where the lactate shuttling is more likely to occur. By considering a photon mapping analogy, we represent glycogen granules as energy sources that emit energy packets, which can be absorbed by the surrounding neurite structures (see figure 3), according to constraints derived from the theoretical mechanisms of neuro-glia metabolic coupling [MA15, BR07]:

- **power source:** the released energy depends on the size of glycogen granules, which are represented as spheres of varying radius (see figure 3). According to our illustrative model, these granules cast energy packets onto the surrounding structures, with a number proportional to its size, and a photon map is computed and stored as a kd-tree [Jen01].
- **energy irradiation:** a restricted set of neurotransmitters and neuromodulators is able to promote glycogenolysis in astrocytes [MA15]. They can be modeled as anisotropic direction-selective energy irradiation modulators, and included as importance maps [PP98] for modulating or blocking the energy emitting directions (indicated in red in figure 3).
- **energy absorption:** the shuttling of derived lactate from astrocyte to neurons is mediated by lactate transporters (MCTs) [Bar13], which can be modeled as anisotropic direction-selective modulators, for energy packets reaching the neurite surface (indicated in green in figure 3).

With respect to the radiance transfer, we implemented an absorption model similar to Lambert-Beer law [CL49] that incorporates a distance-based gaussian decay from each glycogen power source; thereby reflecting the influence of glycogen granules both near and

far to membranes. The constraints are incorporated in the model as modulators or switch functions, affecting both the energy absorption and the irradiation decay. Hence, given a neural process at position $\mathbf{x^p}$ and a glycogen granule energy packet g_i at position $\mathbf{x_i^g}$, we define an absorption rate as:

$$p_\alpha(\mathbf{x^p}, g_i) = K(r_i^g)\lambda^g(\mathbf{x_i^g}, \omega_i^p)\lambda^p(\mathbf{x^p}, \omega_i^p)e^{-\int_{x_i^g}^{x^p}\mu(x)dx}, \quad (1)$$

where $K(r_i^g)$ is the glycogen irradiation power, λ^g is a modulating anisotropy term taking into account the presence of activating enzymes for glycogenolysis, λ^p is a modulating anisotropy term taking into account the presence of enzymes for lactate metabolization, and $\mu(x)$ is the absorption coefficient taking into account the tortuosity for energy transport due to occlusion or friction along the path connecting the glycogen source power to the process. The modulating functions λ^g,λ^p depend also on the irradiation direction ω_i^p. The total energy absorption rate is obtained by summing up the contribution of all glycogen energy packets:

$$p_\alpha(\mathbf{x^p}) = \sum_i p_\alpha(\mathbf{x^p}, g_i). \quad (2)$$

Implementation. We derived a preliminary simplified version of the absorption model by integrating the isotropic emission from granules sources, the isotropic absorption from the neural structures of interest, and the isotropic tortuosity along the path connecting the neurite to the structure of interest. With these components, glycogen granules irradiate in same way along all directions. Energy packets are generated uniformly along the surface of the glycogen granule and stored in a kd-tree. The absorption rate computation is performed on a vertex basis, and accounts for the K-nearest-neighbor (KNN) search distance threshold R by presuming that distant energy packets do not significantly contribute to the absorbed energy of structures (indicated in green in Figure 3). This distance is chosen in a way to be a trade-off between computational workload and the mean length of peripheral astrocytic processes [DHK15] (less than 1 μm). Given the isotropic assumption, both the modulating functions and absorption coefficient become constant, so the equation 2 is simplified to

$$p_\alpha(\mathbf{x^p}) = \sum_i K_i\lambda^g\lambda^p e^{-\mu\|\mathbf{x_i^g}-\mathbf{x^p}\|}, \quad (3)$$

and computed by accumulating all contributions from energy packets in the surrounding area.

4. Results

Dataset	BB (μm)	V(M)	GL	# P(K)	T(m)
Hippocampus1	7.1x6.7x4.7	6.28	1007	135	15.8
Hippocampus2	14x14x24	0.98	9438	38K	25.3
Cortex1	5x5x5	0.66	3037	407	13.8
Cortex2	5x5x5	1.08	7719	110	2.8
Cortex3	5x5x5.9	1.46	4128	546	5.7
Cortex4	5x5x5	2.78	7048	110	6.8

Table 1: ***Processing statistics:*** *dataset size as bounding box (# BB) in microns, number of M vertices (V), number of glycogen granules (GL), number of emitted K packets (P), and the processing time in minutes.*

We tested the absorption model on a series of high resolution 3D reconstructions from rodents brains, and provide a summary of preliminary evaluation performed from domain scientists. Datasets include neural processes, like dendrites, axons, and astrocytes, as well as the intracellular mitochondria. Table 1 provides statistics on data processing, with respect to the model size in terms of bounding box, number of vertices, number of glycogen granules, number of emitted energy packets, and processing time in minutes. For all datasets, we considered $R = 0.5\mu m$ as influence radius for accumulating energy packets contributions and processing times were computed on a laptop equipped with Intel i7-4700HQ 2.4 GHz CPU and 8GB RAM and running Linux Ubuntu kernel 3.13.

4.1. Evaluation.

The computed absorption rates on the datasets of table 1 were log-normalized and color mapped according to a diverging Color Brewer scheme [HB03] (see Figure 4), and integrated with NeuroMorph analysis toolset inside the Blender environment [JNC*15]. The presence of peaks in absorption rates helped domain scientists in finding areas of interest, and performing qualitative visual correlations with surrounding organelles and structures. We report here on some examples of analysis:

- **synaptic plasticity:** in figure 5, glycogen absorption mapping in a portion of the dataset Hippocampus1 showing two dendrites highlights that glycogen could be involved in synaptic plasticity [RB16]. Sites of possible dendritic spines formation (red arrows) and maintenance (green arrows) are found neighboring areas containing high glycogen granules density;
- **mitochondria**: figure 6 shows a small portion of the mouse Somatosensory Cortex1 dataset, highlighting how absorption map peaks (on the left) correlate with the presence of dendritic mitochondria (red arrows on the right), which are the intracellular organelles responsible for the usage of lactate to ultimately synthesize ATP [Bar13];
- **synapses:** figure 7 shows that the glycogen absorption map peaks (on the left) correlate with the presence of an asymmetric (presumably excitatory) shaft synapse; a continuous neurotransmitter release at this site might result in the formation of a spine;
- **boutons and PSDs:** figure 8 shows another example highlighting that absorption map peaks on astrocyte morphology can correlate with the presence of boutons, spines and PSDs, further indicating that glycogen generated energy is fundamental for sustaining neural connections and spines generation;
- **axons:** figure 9 highlights absorption peaks in specific axon bundles in dataset Hippocampus1, conforming the hypothesis that axons uptake glycogen-generated lactate [LTK*16, She17].

These examples show how the absorption model can be successfully employed to test neuroenergetics hypotheses and rapidly investigate the correlation with morphology. In general, domain scientists found absorption maps particularly useful during glycogen analysis for the spatial discrimination capabilities and for reducing clutter and occlusion due to glycogen granules (see figure 10). Moreover, absorption maps can be useful for the comparative analysis of glycogen distribution and astrocyte morphologies, in order to recognize the channels for lactate emission (see figure 11).

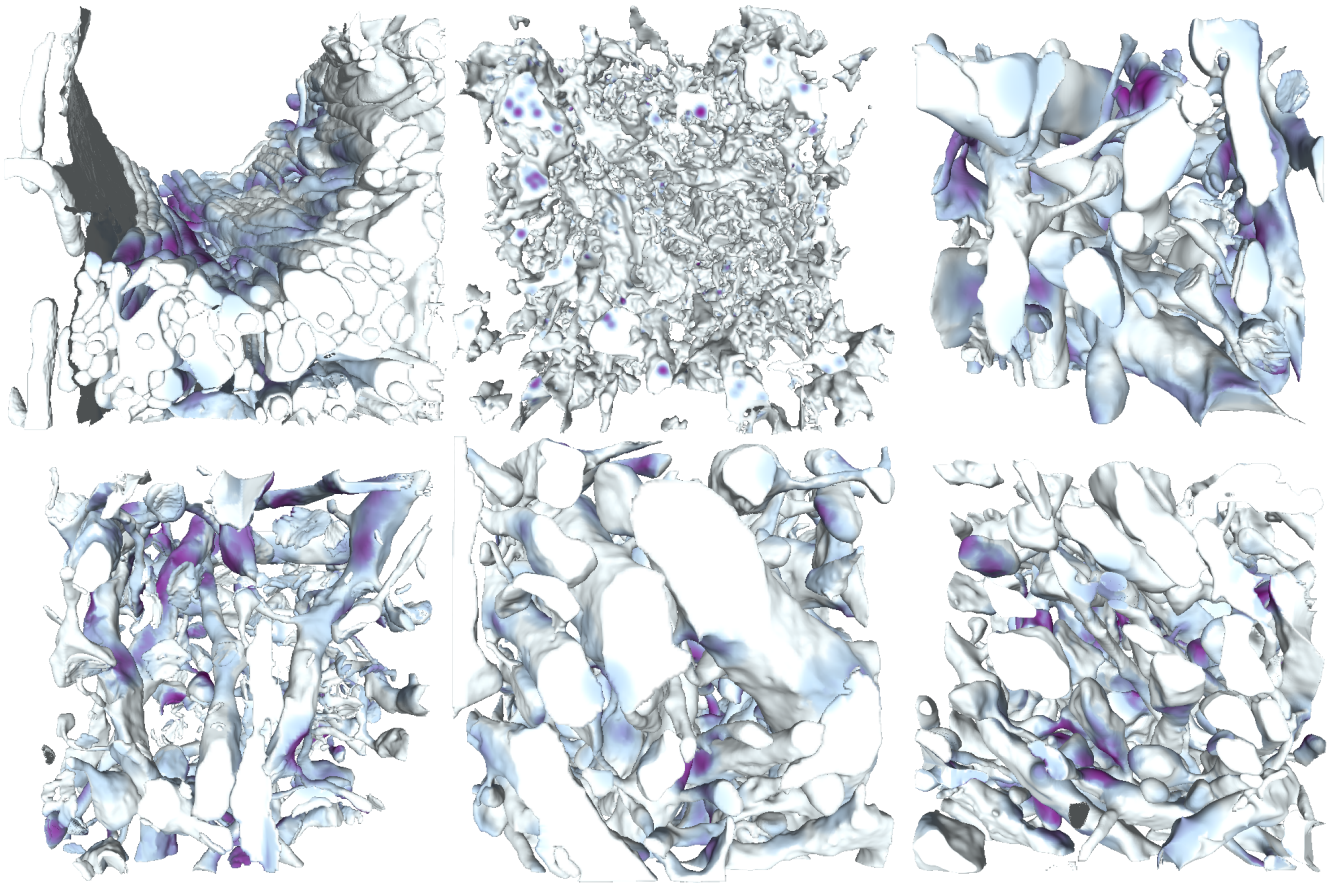

Figure 4: ***Absorption rate maps:*** *color maps of glycogen lactate absorption rate are computed for datasets in table 1 according to a diverging Color Brewer scheme [HB03]. From top left to bottom right, Hippocampus1, Hippocampus2, Cortex 1, Cortex2, Cortex3 and Cortex4. Images produced with Meshlab software [CCC*08].*

Immersive exploration. To evaluate and test the absorption model, we also performed interactive sessions on a fully immersive virtual reality (VR) environment CAVE (cave automatic virtual environment) [CNSD93]. The CAVE space is a cubic room with 3-m sides that are each projected with two 8-megapixel streams. With this setup, several people are able to simultaneously stand inside a 3D model, where details could be magnified on demand and eventually become a million-fold larger (μm to m). The 3D model was projected directly from the 3D modelling Blender window interface by using TechViz software (www.TechViz.net), while the user could manipulate the model inside the room with a controller. A head-tracking system modify the perspective of the object based on the position of the user, who is able to move freely in the room and observe the model from different positions. Figure 12 shows interactive sessions of explorative analysis of hippocampus 2 model together with EM slices rendered with NeuroMorph package [JNC*15]. The peaks in absorption maps over the astrocyte morphology drove domain experts in collaborative discussion and comparison for confirming and formulating hypothesis on lactate shuttling mechanisms and usage of glycogen generated energy.

5. Conclusions

We presented a simplified illustrative model of glycogen absorption targeted at visual investigation of neural morphology and for hypothesis testing about glycogen utilization. This could be useful to assess whether difference in energy consumption exist for instance during physiological conditions, aglycemia or for memory formation. Current limitations are related to the difficulties in deriving the parameters from neuroenergetics entities for precisely modeling of the machinery involved in lactate transport. However, given the encouraging results of our preliminary evaluation, we plan to incorporate more precise scattering and absorption constraints by processing data coming from in-vivo and in-vitro lactate transporters acquisition [CFM*08]. Furthermore, the glycogen lactate absorption computation is currently integrated into a visual analysis workflow for morphology investigations [JNC*15]. However, a limitation of the whole pipeline is that it requires a previously reconstructed 3D model, which takes a considerable amount of time and effort to process. Finally, we believe that the pattern of glycogen distribution can provide significant cues for morphology discrimination, and that the usage of an irradiation energy scheme can provide hints for visual understanding of neural morphology

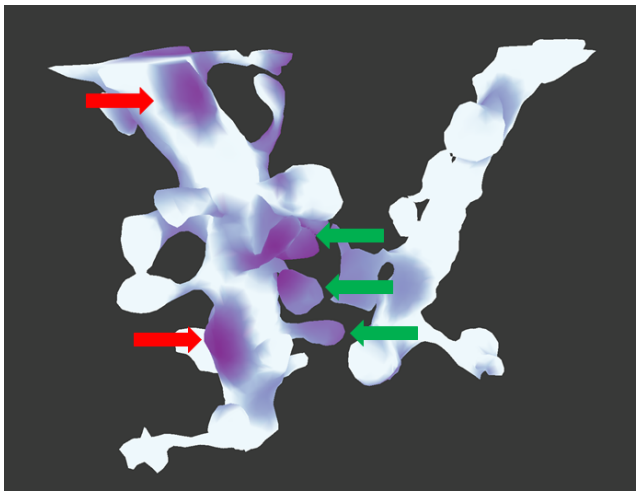

Figure 5: ***Synaptic plasticity:*** *the analysis of absorption map highlighted the presence of shaft synapses, from which spines can generate (red arrows), and highly plastic small-size dendritic spines (green arrows). Dendrite detail from from dataset Hippocampus1, rendered within Blender environment.*

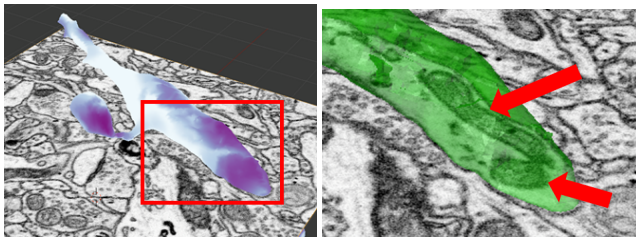

Figure 6: ***Correlation with mitochondria:*** *the peaks of glycogen lactate absorption maps (left) are correlated with mitochondria (red arrows on the right). Dendrite detail from dataset Somatosensory Cortex1. Images produced with Blender and Neuromorph softwares [JNC*15].*

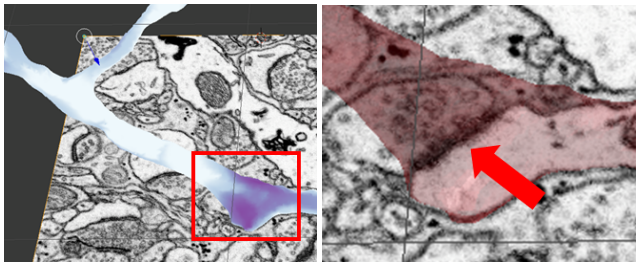

Figure 7: ***Correlation with synapse:*** *the peaks of glycogen lactate absorption maps (left) are correlated with the presence of a shaft synapse (red arrow on the right). Axon detail from dataset Somatosensory Cortex2. Images produced with Blender and Neuromorph softwares [JNC*15].*

evolution. We plan to integrate the absorption model in a real-time scalable volume ray casting framework for directly rendering raw

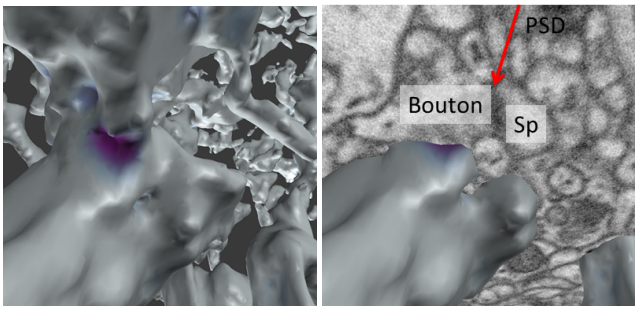

Figure 8: ***Correlation with PSD:*** *the peak of glycogen lactate absorption map on astrocyte morphology is correlated with the presence of a PSD and a bouton (on the right). Astrocyte detail from dataset Hippocampus2. Images produced with Blender and Neuromorph softwares [JNC*15].*

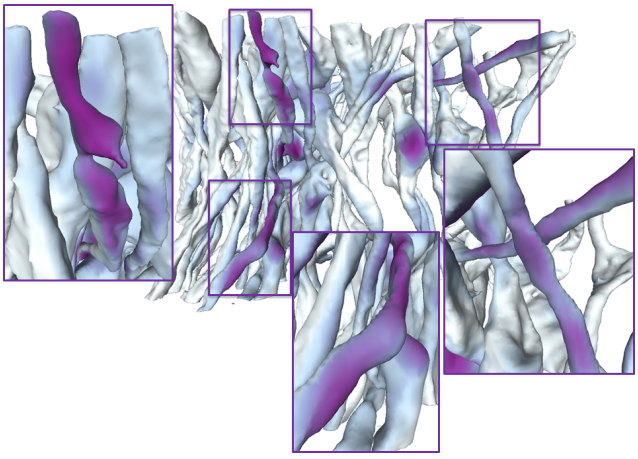

Figure 9: ***Correlation with axons:*** *the peaks of absorption map show that specific bundle of axons exhibit high lactate absorption rate. Axons details from dataset Hippocampus 1. Images produced with Meshlab software [CCC*08].*

SEM image stacks [HAAB*17] and in systems for real time exploration of abstract representations of brain structures [MAAB*17].

Acknowledgements. We thank Kalpana Kare and Daniya Boges for the technical support for the 3D reconstruction pipelines and coding; the KVL team for the support in the use of CAVE and for providing computing clusters to process the image stacks for 3D reconstructions; Graham Knott and the BioEM Facility at EPFL (Lausanne, Switzerland), and Elena Vezzoli from University of Milano (Milano, Italy), for providing the EM stacks that we used for extracting the 3D models. This work was supported by the KAUST Grant *KAUST-EPFL Alliance for Integrative Modeling of Brain Energy Metabolism* to Pierre Magistretti and Henry Markram.

References

[ACW*15] ASADULINA A., CONZELMANN M., WILLIAMS E. A., PANZERA A., JÉKELY G.: Object-based representation and analysis of light and electron microscopic volume data using blender. *BMC bioinformatics 16*, 1 (2015), 229. 2

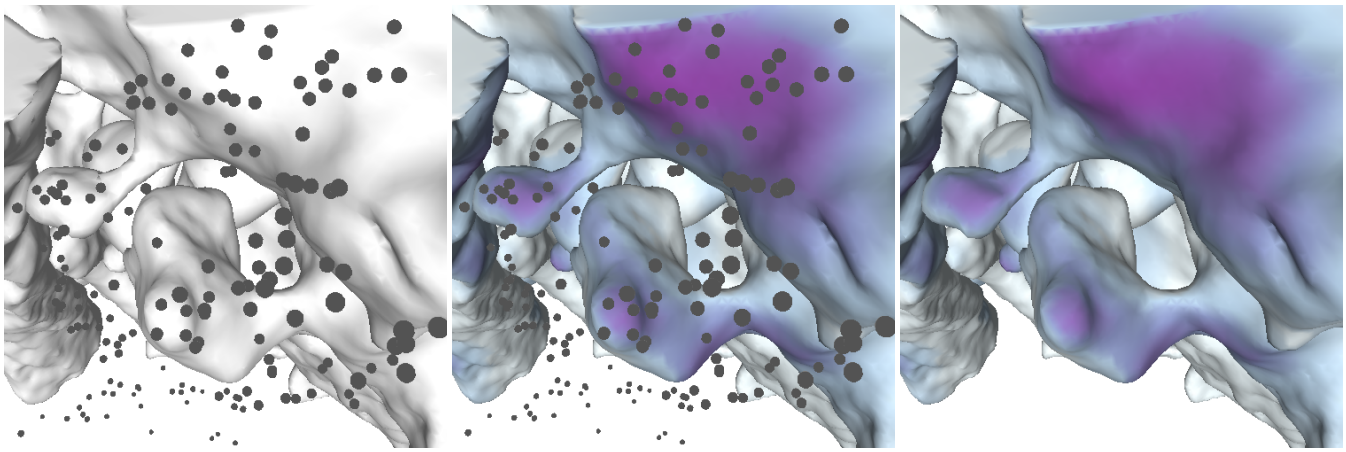

Figure 10: ***Glycogen analysis:*** *domain scientists perform analysis of glycogen distribution compared to neuron morphologies (left). Absorption maps help analysis in spatial discrimination (center), and reduce clutter due to glycogen granules (right). Dendrite detail from dataset Hippocampus1. Images produced with Meshlab software [CCC*08].*

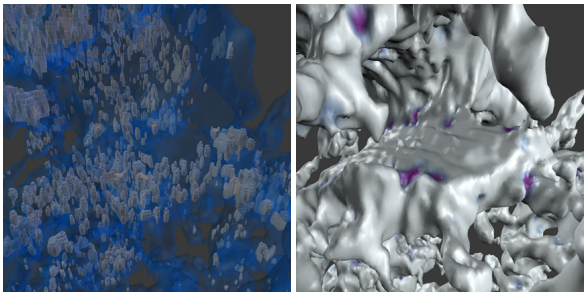

Figure 11: ***Astrocyte glycogen analysis.*** *Left: glycogen analysis in astrocyte is particularly complex since transparent morphologies clutter and reduce spatial discrimination. Right: absorption map in astrocyte surface provide indication of the most probable channels for lactate shuttling. Dataset Hippocampus2 rendered inside Blender environement.*

[AMB*17] AGUS M., MARTON F., BETTIO F., HADWIGER M., GOBBETTI E.: Data-driven analysis of virtual 3D exploration of a large sculpture collection in real-world museum exhibitions. *ACM Journal on Computing and Cultural Heritage* (2017). To appear. 3

[BAAK*13] BEYER J., AL-AWAMI A., KASTHURI N., LICHTMAN J. W., PFISTER H., HADWIGER M.: Connectomeexplorer: Query-guided visual analysis of large volumetric neuroscience data. *IEEE Trans. on Vis. and Comp. Graph. 19*, 12 (2013), 2868–2877. 2

[BAM11] BÉLANGER M., ALLAMAN I., MAGISTRETTI P. J.: Brain energy metabolism: focus on astrocyte-neuron metabolic cooperation. *Cell metabolism 14*, 6 (2011), 724–738. 2

[Bar13] BARROS L. F.: Metabolic signaling by lactate in the brain. *Trends in neurosciences 36*, 7 (2013), 396–404. 3, 4

[BBH15] BERNING M., BOERGENS K. M., HELMSTAEDTER M.: Segem: efficient image analysis for high-resolution connectomics. *Neuron 87*, 6 (2015), 1193–1206. 2

[BH16] BORRETT S., HUGHES L.: Reporting methods for processing and analysis of data from serial block face scanning electron microscopy. *Journal of microscopy* (2016). 2

[BR07] BROWN A. M., RANSOM B. R.: Astrocyte glycogen and brain energy metabolism. *Glia 55*, 12 (2007), 1263–1271. 3

[CBB*16] CALÌ C., BAGHABRA J., BOGES D. J., HOLST G. R., KRESHUK A., HAMPRECHT F. A., SRINIVASAN M., LEHVÄSLAIHO H., MAGISTRETTI P. J.: 3D immersive virtual reality for studying cellular compartments in 3D models from EM preparations of neural tissues. *Journal of Comparative Neurology 524*, 1 (2016), 23–38. 1, 2

[CCC*08] CIGNONI P., CALLIERI M., CORSINI M., DELLEPIANE M., GANOVELLI F., RANZUGLIA G.: MeshLab: an Open-Source Mesh Processing Tool. In *Eurographics Italian Chapter Conf.* (2008). 5, 6, 7

[CFM*08] CHIRY O., FISHBEIN W. N., MEREZHINSKAYA N., CLARKE S., GALUSKE R., MAGISTRETTI P. J., PELLERIN L.: Distribution of the monocarboxylate transp. MCT2 in human cerebral cortex: an immunohistochemical study. *Brain research 1226* (2008), 61–69. 5

[CL49] COMMONER B., LIPKIN D.: The application of the beer-lambert law to optically anisotropic systems. *Science 110*, 2845 (1949). 3

[CMS*09] CALÃŇ C., MARCHALAND J., SPAGNUOLO P., GREMION J., BEZZI P.: Chapter 20 regulated exocytosis from astrocytes. *International Review of Neurobiology 85* (2009), 261 – 293. 2

[CNSD93] CRUZ-NEIRA C., SANDIN D. J., DEFANTI T. A.: Surround-screen projection-based virtual reality: the design and implementation of the cave. In *Proceedings of the 20th annual conference on Computer graphics and interactive techniques* (1993), ACM, pp. 135–142. 5

[CSS*12] CARDONA A., SAALFELD S., SCHINDELIN J., ARGANDA-CARRERAS I., PREIBISCH S., LONGAIR M., TOMANCAK P., HARTENSTEIN V., DOUGLAS R. J.: Trakem2 software for neural circuit reconstruction. *PloS one 7*, 6 (2012), e38011. 2

[DHK15] DEROUICHE A., HASELEU J., KORF H.-W.: Fine astrocyte processes contain very small mitochondria: glial oxid. capability may fuel transmitter metabolism. *Neurochem. Res. 40* (2015), 2402–2413. 4

[GHF07] GODDARD T. D., HUANG C. C., FERRIN T. E.: Visualizing density maps with {UCSF} chimera. *Journal of Structural Biology 157*, 1 (2007), 281 – 287. Software tools for macromolecular microscopy. 3

[GHLG15] GAO J. S., HUTH A. G., LESCROART M. D., GALLANT J. L.: Pycortex: an interactive surface visualizer for fmri. *Frontiers in Neuroinformatics 9* (2015), 23. 3

[HAAB*17] HADWIGER M., AL-AWAMI A., BEYER J., AGUS M., PFISTER H.: Sparseleap: Efficient empty space skipping for large-scale volume rendering. *Proc. of IEEE Visualization* (2017). To appear. 6

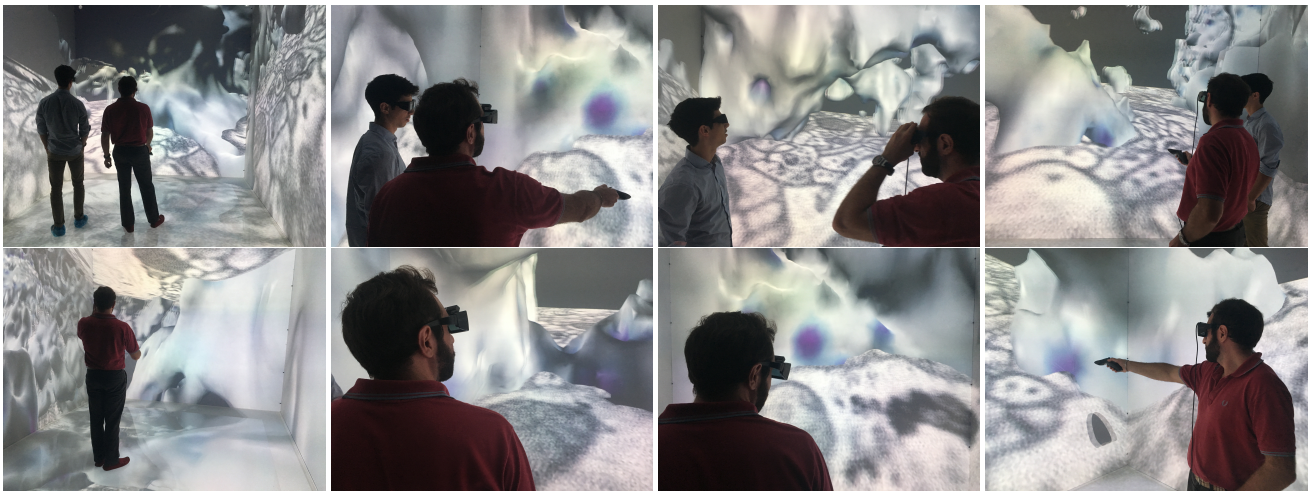

Figure 12: ***Immersive sessions:*** *the absorption model has been integrated into an interactive virtual reality environment for real time exploration of morphologies. Here the exploration of astrocyte morphology of dataset Hippocampus2 is shown.*

[HB03] HARROWER M., BREWER C. A.: Colorbrewer. org: an online tool for selecting colour schemes for maps. *The Cartographic Journal 40*, 1 (2003), 27–37. 4, 5

[JC95a] JENSEN H. W., CHRISTENSEN N. J.: Efficiently rendering shadows using the photon map. In *Proceedings of Compugraphics '95* (1995), pp. 285–291. 3

[JC95b] JENSEN H. W., CHRISTENSEN N. J.: Photon maps in bidirectional monte carlo ray tracing of complex objects. 215–224. 3

[Jen96] JENSEN H. W.: Global illumination using photon maps. In *Proceedings of the Eurographics Workshop on Rendering Techniques '96* (London, UK, UK, 1996), Springer-Verlag, pp. 21–30. 3

[Jen01] JENSEN H. W.: *Realistic image synthesis using photon mapping*, vol. 364. Ak Peters Natick, 2001. 3

[JNC*15] JORSTAD A., NIGRO B., CALI C., WAWRZYNIAK M., FUA P., KNOTT G.: Neuromorph: a toolset for the morphometric analysis and visualization of 3d models derived from electron microscopy image stacks. *Neuroinformatics 13*, 1 (2015), 83–92. 2, 4, 5, 6

[KMM*13] KANDEL E. R., MARKRAM H., MATTHEWS P. M., YUSTE R., KOCH C.: Neuroscience thinks big (and collaboratively). *Nature Reviews Neuroscience 14*, 9 (2013), 659–664. 1

[KMWL08] KNOTT G., MARCHMAN H., WALL D., LICH B.: Serial section scanning electron microscopy of adult brain tissue using focused ion beam milling. *The Journal of Neurosc. 28*, 12 (2008), 2959–2964. 2

[KVRKB*15] KAYNIG V., VAZQUEZ-REINA A., KNOWLES-BARLEY S., ROBERTS M., JONES T. R., KASTHURI N., MILLER E., LICHTMAN J., PFISTER H.: Large-scale automatic reconstruction of neuronal processes from electron microscopy images. *Medical Image Analysis 22*, 1 (2015), 77 – 88. 2

[LNT*08] LAU C., NG L., THOMPSON C., PATHAK S., KUAN L., JONES A., HAWRYLYCZ M.: Exploration and visualization of gene expression with neuroanatomy in the adult mouse brain. *BMC Bioinformatics 9*, 1 (2008), 153. 3

[LTK*16] LEWIS T. L., TURI G. F., KWON S.-K., LOSONCZY A., POLLEUX F.: Progressive decrease of mitochondrial motility during maturation of cortical axons in vitro and in vivo. *Current Biology 26*, 19 (2016), 2602–2608. 4

[MA15] MAGISTRETTI P. J., ALLAMAN I.: A cellular perspective on brain energy metabolism and functional imaging. *Neuron 86*, 4 (2015), 883–901. 1, 2, 3

[MAAB*17] MOHAMMED H., AL-AWAMI A., BEYER J., CALI C., MAGISTRETTI P., PFISTER H., HADWIGER M.: Abstractocyte: A visual tool for exploring nanoscale astroglial cell morphology. *Proceedings of IEEE Visualization* (2017). To appear. 6

[MWE*16] MÄCHLER P., WYSS M. T., ELSAYED M., STOBART J., GUTIERREZ R., VON FABER-CASTELL A., KAELIN V., ZUEND M., SAN MARTÍN A., ROMERO-GÓMEZ I., ET AL.: In vivo evidence for a lactate gradient from astrocytes to neurons. *Cell metabolism 23*, 1 (2016), 94–102. 2

[OBA*16] OE Y., BABA O., ASHIDA H., NAKAMURA K. C., HIRASE H.: Glycogen distribution in the microwave-fixed mouse brain reveals heterogeneous astrocytic patterns. *Glia 64*, 9 (2016), 1532–1545. 2

[PKB*12] PFISTER H., KAYNIG V., BOTHA C. P., BRUCKNER S., DERCKSEN V. J., HEGE H., ROERDINK J. B. T. M.: Visualization in connectomics. *CoRR abs/1206.1428* (2012). 2

[PP98] PETER I., PIETREK G.: Importance driven construction of photon maps. In *Rendering Techniques*. Springer, 1998, pp. 269–280. 3

[RB16] RICH L., BROWN A. M.: Glycogen multiple roles in the cns. *The Neuroscientist* (2016), 1073858416672622. 4

[She17] SHENG Z.: The interplay of axonal energy homeostasis and mitochondrial trafficking and anchoring. *Trends in Cell Biol.* (2017). 4

[SMGL*16] SCHNEIDER-MIZELL C. M., GERHARD S., LONGAIR M., KAZIMIERS T., LI F., ZWART M. F., CHAMPION A., MIDGLEY F. M., FETTER R. D., SAALFELD S., ET AL.: Quantitative neuroanatomy for connectomics in drosophila. *Elife 5* (2016), e12059. 2

[SSB*11] SUZUKI A., STERN S. A., BOZDAGI O., HUNTLEY G. W., WALKER R. H., MAGISTRETTI P. J., ALBERINI C. M.: Astrocyte-neuron lactate transport is required for long-term memory formation. *Cell 144*, 5 (2011), 810–823. 2

[SSKH11] SOMMER C., STRAEHLE C., KÖTHE U., HAMPRECHT F. A.: Ilastik: Interactive learning and segmentation toolkit. In *2011 IEEE international symposium on biomedical imaging: From nano to macro* (2011), IEEE, pp. 230–233. 2

[TG16] TITZE B., GENOUD C.: Volume scanning electron microscopy for imaging biological ultrastructure. *Biology of the Cell* (2016). 1

[XWH13] XIA M., WANG J., HE Y.: Brainnet viewer: A network visualization tool for human brain connectomics. *PLOS ONE 8*, 7 (07 2013), 1–15. 3